

Microbial carbon processing in oligotrophic Lake Lucerne (Switzerland): results of in situ ^{13}C -labelling studies

J. M. Lammers · C. J. Schubert · J. J. Middelburg · G. J. Reichart

Received: 8 January 2017 / Accepted: 15 September 2017 / Published online: 23 October 2017
© The Author(s) 2017. This article is an open access publication

Abstract Although lakes play a major role in the storage of organic carbon, processes involved are not yet very well characterized, especially for oligotrophic lakes. Whether a lake functions as a net source or sink for carbon depends on relative rates of primary production, inputs of terrestrial organic matter and respiration. The microbial community will affect the efficiency of carbon cycling and thereby potential carbon storage. Because the organic matter fluxes are smaller in oligotrophic lakes they have been studied less intensively with respect to their carbon cycling compared to eutrophic lakes. Whether they play an appreciable role in freshwater carbon cycling relies on unraveling primary and secondary production. Here we present the results from such a study in oligotrophic Lake

Lucerne, Switzerland. Based on in situ carbon isotopic labelling experiments using dark, glucose-labelled and transparent, DIC-labelled bottles positioned at different depths in the water column, we conclude that even though the photic zone was very deep, integrated primary productivity was consistently low. The carbon processing efficiency of the heterotrophic producers was such that photosynthesized organic matter was fully consumed, even during times of maximum productivity. This implies that the heterotrophic producers were well adapted to rapidly respond to a temporary increase in primary productivity, which is in line with calculated bacterial growth efficiencies in the surface water layer. Highest glucose-based productivity, as a measure of the heterotrophic potential, was observed in the deepest parts of the water column. Chemoautotrophy was shown at 60 m water depth and is of relatively minor importance for overall fluxes. Mixotrophy was recognized as a strategy to keep up production when light conditions become less favorable for autotrophic growth. A mesocosm experiment earlier in the year indicated lower primary production, which agrees well with the timing of this experiment preceding the annual spring bloom. During the low-productivity season the coupling between phytoplankton and bacterial production was much weaker and potentially more organic matter could escape recycling at that time, although quantitatively fluxes remained very low.

Responsible Editor: Jack Brookshire.

J. M. Lammers · J. J. Middelburg · G. J. Reichart (✉)
Department of Earth Sciences, Utrecht University,
P.O. Box 80.021, 3508 TA Utrecht, The Netherlands
e-mail: g.j.reichart@nioz.nl

C. J. Schubert
Department of Surface Waters - Research and
Management, Eawag - Swiss Federal Institute of Aquatic
Science and Technology, Seestrasse 79,
6047 Kastanienbaum, Switzerland

G. J. Reichart
Department of Ocean Systems, NIOZ Royal Netherlands
Institute for Sea Research, P.O. Box 59,
1790 AB Den Burg, Texel, The Netherlands

Keywords Lacustrine food-web · Phytoplankton-
bacteria coupling · $\delta^{13}\text{C}$ tracer · Biomarkers

Introduction

The cycling of carbon in inland waters is probably one of the least constrained compartments of the global carbon cycle (Battin et al. 2009; Heimann 2009). Lakes play a major role in the terrestrial carbon cycle as sites of primary production and processing of organic matter, and are not just conduits of terrestrial carbon to oceans (Cole et al. 2007; Tranvik et al. 2009; Raymond et al. 2013; Weyhenmeyer et al. 2015). In general, the degree to which in situ production or allochthonous organic matter contributes to secondary production differs for individual lakes, with the impact on global carbon cycling still being under debate (Pace et al. 2004; Brett et al. 2009; Cole et al. 2011; Brett et al. 2012).

Many of the world's largest lakes are oligotrophic and can be found from southern Siberia (Lake Baikal) to North America (Lake Superior, Lake Michigan, Lake Huron) and Africa (Lake Malawi, Lake Tanganyika) (www.globalgreatlakes.org). Together these lakes make up roughly 50% of world's freshwater supply, making them crucially important for the supply of drinking water. They are also important in terms of biodiversity, ecology, economics and public service. These lakes do not only affect climate on a regional scale through heat and water exchange with the atmosphere, but they may also be important players in the global carbon cycle (Cole et al. 2007). For unproductive systems, it has been suggested that respiration often exceeds primary production, resulting in CO₂ diffusion to the atmosphere (Del Giorgio et al. 1997). Whereas eutrophic lakes are important because of the high volumetric rates of carbon cycling, oligotrophic lakes may play an important role for the carbon cycle as well, as such lakes can be of appreciable size, up to hundreds of square kilometers. Furthermore, studies targeting food webs and organic matter processing in these oligotrophic lakes are needed to quantify their potential role in the processing of terrestrial carbon.

Although smaller than some of the afore-mentioned lakes, Lake Lucerne, Switzerland, is an example of a large, oligotrophic lake. Lake Lucerne is a hard-water lake with a volume of 11.8 km³. It has returned to an oligotrophic state (since 1989) after a brief period of eutrophication (1970–1977), with current total (dissolved) phosphorous concentrations ranging between 5 and 10 mg m⁻³ and nitrate-nitrogen concentrations

of 600–700 mg m⁻³ (Bürgi and Stadelmann 2002). Plankton communities and food-web structure and functioning have been studied in Lake Lucerne, mainly in the context of changes in trophic conditions (Bloesch et al. 1977; Bürgi et al. 1999; Bürgi and Stadelmann 2002). Currently the lake is considered well restored with recovered species diversity and evenness, although the species composition is still different from the pre-eutrophication period (Bürgi and Stadelmann 2002).

In lakes coupling between primary and secondary production is important because of the potential impact on carbon recycling or storage. Strong coupling between phytoplankton and heterotrophic bacteria results in efficient remineralization of photosynthesized organic matter and hence in recycling of carbon. When substantial time lags exist between bacterial responses to phytoplankton production, dead organic matter may escape bacterial degradation in surface water, resulting in export to deeper water. Investigating these processes requires the accurate targeting of the organisms involved. Here we present a study on the relative importance of primary versus glucose-based heterotrophic production and respiration in Lake Lucerne. The aim of this research is to unravel the organic carbon dynamics in a oligotrophic lake, whereas at the same time investigating the potential role of allochthonous organic matter on the food web. We use ¹³C as a deliberate tracer to follow carbon flows and use label incorporation into specific phospholipid-derived fatty acids (PLFA) to distinguish between different groups of microbial primary producers (photoautotrophic, mixotrophic and chemoautotrophic) and secondary producers (heterotrophic bacteria). This allowed us to investigate group-specific primary production, the depth distribution of various primary producers and carbon transfer from primary producers to heterotrophic bacteria. These data are used to investigate whether organic carbon production and consumption are balanced in this oligotrophic lake.

Materials and methods

Study site

Experiments were carried out in Lake Lucerne, a large, oligotrophic prealpine lake in Switzerland (Fig. 1).

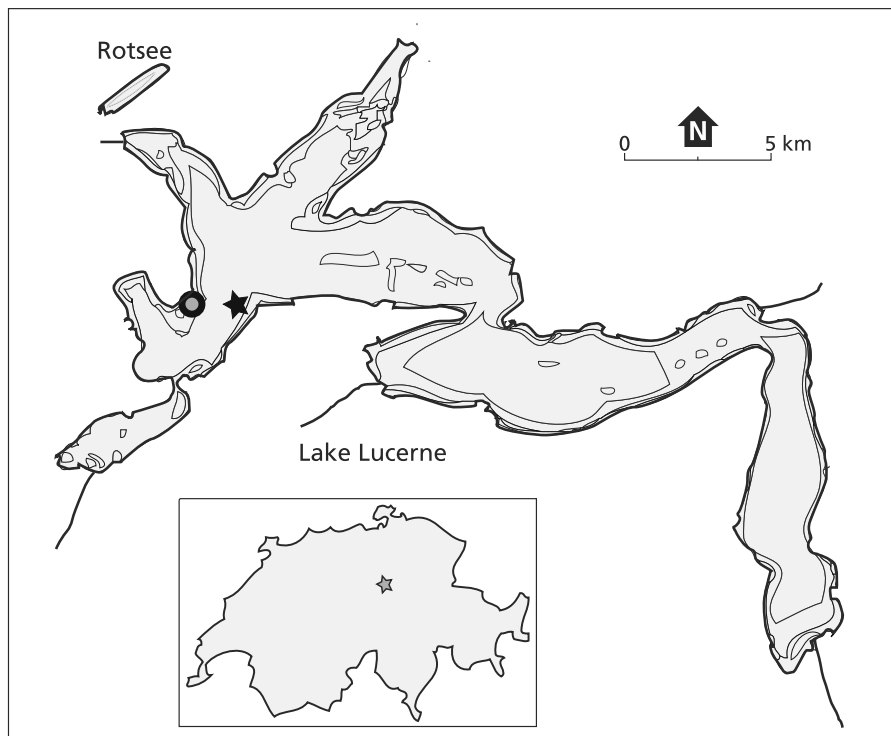


Fig. 1 Map showing the location of Lake Lucerne and its major in- and outflowing rivers. The smaller insert showing location of lake Lucerne in Switzerland. The location of the 2011 bottle

experiments is indicated by a star in the figure of Lake Lucerne; the 2012 mesocosm experiment is indicated by a circle

Lake Lucerne is located 434 m above sea level, has a surface area of 113 km², a mean depth of 104 m and a maximum depth of 214 m. The lake water has a residence time of 3.4 years and the lake itself is oligomictic with complete overturn occurring on average every 6 years. The total catchment area of the lake is 2124 km², with four major rivers flowing into Lake Lucerne: Reuss, Muota, Engelberger Aa and Sarner Aa, together contributing ~ 80% of the lakes water supply. Dominating phytoplankton during summer are pennate diatoms, chrysophyte algae and cryptophyte algae, while *Rhodomonas* (Cryptophyta) and centric diatoms dominate during winter (Bossard et al. 2001).

Experimental approach

To elucidate the carbon flow within the microbial down we use polar-derived fatty acids (PLFAs). These are cell membrane constituents (lipids) that are produced by a wide variety of organisms as they are an essential component of all microbes and hence

represent a wide range of feeding types. PLFAs represent viable biomass, since they are hydrolyzed within minutes to hours after cell lysis, releasing the polar head groups (White et al. 1979). Although PLFAs are rarely unique for specific source organisms, they have been successfully applied in trophic studies e.g. to differentiate between producers such as chemoautotrophic, photoautotrophic and mixotrophic phytoplankton and heterotrophic bacteria (van Oevelen et al. 2006; van Gaever et al. 2009; De Kluijver et al. 2010). Using labeled ¹³C-bicarbonate or ¹³C-glucose allows distinguishing between chemoautotrophic and heterotrophic produced PLFAs. Photoautotrophic or chemoautotrophic production leads to PLFA ¹³C-enrichment in bicarbonate-labelled incubations, while heterotrophic production can be detected via PLFA ¹³C-enrichment under glucose-labelled incubations.

Incubation experiments and sample collection

In 2011, an in situ ^{13}C -labelling experiment was carried out from June 16 to June 20. The bottle experiments in Lake Lucerne were located near the edge of the Chrüztrichter Basin. This location is relatively far away from major in- or outflowing rivers and has limited direct input of allochthonous organic matter (Blaga et al. 2011). To facilitate comparison of flux rates the experimental location was selected close to a previous sediment trapping study (Blaga et al. 2011). Using Niskin bottles, twelve 25-l bottles were filled with lake water from 6 different depths (5, 10, 20, 40, 60 and 75 m). Using a tube the water was quickly transferred from Niskin to incubation bottles. For each depth, a transparent (polycarbonate) bottle was labelled with ^{13}C -bicarbonate (6.6 mg NaHCO_3 per bottle, > 98 atom% ^{13}C) and a (Low Density Polyethylene) bottle covered in waterproof reflecting aluminum tape was labelled with ^{13}C -glucose (1.6 mg > 99 atom% ^{13}C). Label addition increased DIC and DOC concentrations by 0.16 and $\sim 1\%$ respectively. To unravel the primary and secondary productivity and chemoautotrophy, transparent and dark bottles were attached side by side to a cable connecting an anchor at the lake floor to a buoy at the water–air interface, so that the bottles were placed at the original water depth (Fig. 2). This setup was left in situ for 4 days. At the start of the experiment, in situ oxygen, temperature, conductivity and pH were measured using a CTD probe (Seabird SBE19). At the start (T_0) and end (T_4) of the experiment, samples were taken for dissolved organic carbon (DOC), dissolved



Fig. 2 Setup of the 2012 mesocosm labelling experiment

inorganic carbon (DIC), suspended particulate matter (SPM, bulk organic carbon and lipid biomarkers), and PLFA stable carbon isotope analyses (see below for details on sample collection).

In view of the limited duration of the bottle experiments (4-days), a longer 16-day mesocosm experiment was carried out early spring 2012, using ^{13}C -bicarbonate as a tracer. The mesocosm experiment was executed at the opposite side of the basin compared to the bottle experiments. This site was much shallower and shielded the setup from waves and wind. The ten-meter-deep mesocosm (1 m diameter, 7800 l, Fig. 3) was deployed from March 22 to April 6 (16 days). The mesocosm consisted of a metal frame with floats and a black synthetic bag suspended from the frame. The frame was anchored to the lake floor. The rim of the mesocosm was positioned 1 m above the lake level to avoid exchange of surface water with the lake during the experiment. The experiment was performed earlier in the year compared to the 2011 incubations, both in an attempt to capture the onset of the spring bloom and also for logistical reasons. Samples were taken at 2.5 m water depth within the mesocosm. In situ oxygen concentrations, temperatures and pH were measured using a CTD probe (Seabird SBE19) at T_0 , T_4 , T_7 , T_{11} and T_{14} , when samples were also collected for alkalinity. Label (NaHCO_3 , > 98 atom% ^{13}C) was added between T_0 and T_1 . Samples for DIC and particulate organic carbon (POC) were collected daily for the first 8 days and at T_{11} and T_{15} . Samples for lipid biomarker analyses were collected daily for the first 7 days and at T_{15} .

For analyses of concentrations and stable carbon isotope composition of DOC, samples were filtered over GM/F filters ($0.45\ \mu\text{m}$) and stored frozen ($-20\ ^\circ\text{C}$) in clean vials until further analysis. Samples for DIC were collected without air in 20 ml headspace vials and sealed using air tight caps preventing further microbial activity by mercury chloride poisoning. Samples were stored in the dark and upside down. For SPM, the remaining water from the bottles was filtered over $0.7\ \mu\text{m}$ GF/F filters (pre-weighed and pre-combusted). Filters were stored frozen ($-20\ ^\circ\text{C}$) until extraction.

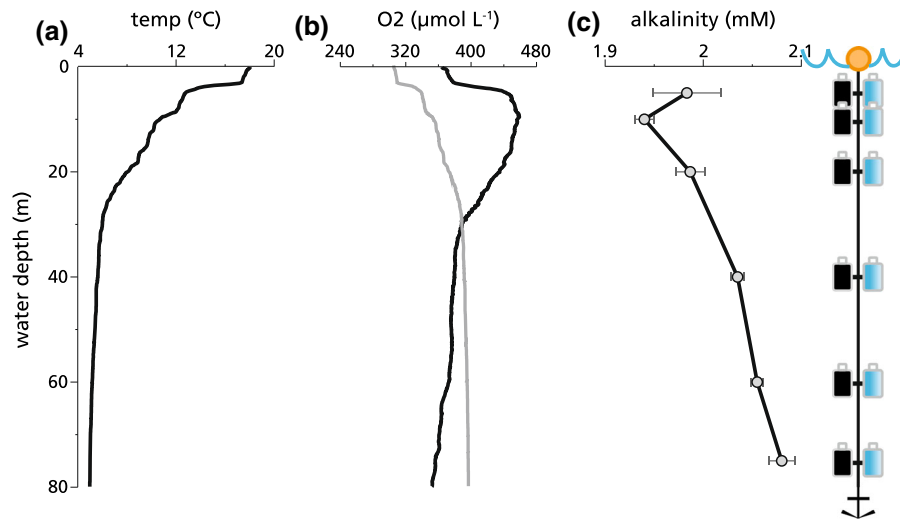


Fig. 3 Physical parameters measured during the (2011) bottle experiment: **a** Temperature in °C, **b** dissolved oxygen concentration in $\mu\text{mol L}^{-1}$ as measured (black line) and the saturation concentration (grey line), and **c** alkalinity in mM.

Laboratory analyses

Alkalinity was determined on 50 ml of water by potentiometric titration with 0.01 M HCl, monitoring pH and using a Gran plot. For the bottle-experiment alkalinity was analyzed for each depth and values represent averages of T_0 and T_4 from light and dark incubations. Samples for the analyses of concentrations and $\delta^{13}\text{C}$ DOC were first acidified, then flushed with helium (removing DIC) and finally oxidized (using peroxodisulfates). DOC samples were then analyzed following (Boschker et al. 2008), using high-performance liquid chromatography-isotope ratio mass spectrometry (HPLC-IRMS, Thermo Surveyor system coupled to a Delta V Advantage using and LC-Isolink interface). DIC concentrations of water samples were measured on a Shimadzu TOC-5050A Carbon analyzer, using an in-house seawater standard. For carbon stable isotope analyses of DIC a helium headspace was made over the DIC samples, which were subsequently acidified using a H_3PO_4 solution. The $\delta^{13}\text{C}$ values of the resulting CO_2 -gas were then measured using a gas bench coupled on line to an IRMS (Thermo Delta V advantage). Using in-house (Na_2CO_3) and international (Li_2CO_3) standards, $\delta^{13}\text{C}_{\text{DIC}}$ was calibrated to the Vienna Peedee Belemnite (V-PDB) scale. Filters for SPM were freeze dried and concentrations and stable carbon isotopic

Alkalinity concentrations are average values of T_0 and light and dark incubations. The bottles correspond to the depths they were deployed at

composition of particulate organic carbon (POC) were measured on small pieces (6–13 circles of 5 mm diameter) cut from these filters. POC concentrations were measured using an elemental analyzer (EA) (Fisons Instruments NA1500), with the $\delta^{13}\text{C}$ being analyzed with the online coupled IRMS (Thermo Deltaplus). Precision was better than 0.35‰ based on in-house standards (Graphite quartzite and Nicotinamide). The relative small amounts of material did not permit true replication, but consistent trends confirm that the internal precision is representative. Concentrations of the organic and inorganic carbon pools showed no systematic changes during incubations and are hence reported as the averages of T_0 and T_4 of both bicarbonate-labelled and glucose-labelled incubations.

Lipids were extracted from the remainders of the freeze-dried SPM filters according to a modified Bligh and Dyer extraction method, which was followed by separation into simple lipid (SL), glycolipid (GL) and phospholipid (PL) fractions based on polarity (Dickson et al. 2009). Phospholipid-derived fatty acids in the PL fractions were converted to fatty acid methyl esters (PL-FAMES) by mild alkaline transmethylation (White et al. 1979) and internal standards were added ($\text{C}_{12:0}$ and $\text{C}_{19:0}$ FAMES). For the 2011 (bottle incubation) samples, concentrations and carbon isotopic composition of the individual FAMES were

determined using gas chromatography combustion isotope ratio mass spectrometry (GC-C-IRMS), following (Middelburg et al. 2000). Concentrations and $\delta^{13}\text{C}$ of PL-FAMES from the mesocosm experiment were determined using a different setup. Concentrations were analyzed using a gas chromatograph (HP 6890) with Helium as carrier gas set at constant pressure and fitted with a flame ionization detector (FID) and a VF-23 ms column (0.25 mm i.d.). Similar as for bulk carbon, concentrations of grouped-PLFAs did not show systematic changes and are shown as the averages of T_0 and T_4 of both bicarbonate-labelled and glucose-labelled incubations. Mass spectrometry was performed using a Thermo Trace GC Ultra, with Helium set at constant flow. Compounds were identified based on retention times and mass spectra and double-bond positions were determined after derivatization with dimethyl-disulfide (DMDS). DMDS was activated with iodine in diethyl ether at 40 °C overnight (Buser et al. 1983). Compound specific $\delta^{13}\text{C}$ values of the mesocosm PL-FAMES were determined using GC-C-IRMS with a ThermoFinnigan Delta Plus XP, using the same type of column as for GC-FID analyses. Oven programming of GC-FID, GC-MS and GC-C-IRMS followed Middelburg et al. (2000). For all PLFAs, values are reported in ‰ versus V-PDB and were corrected for the added carbon atom during methylation. Carbon isotopic values of the derivatizing agents were determined offline.

Data analyses

From the incorporation of ^{13}C into carbon pools (DIC, DOC, POC) and PLFAs, production rates (in $\text{mol L}^{-1} \text{day}^{-1}$) were calculated following (De Kluijver et al. 2013):

$$\text{Production rate} = \frac{\Delta^{13}F_{\text{produced}}}{\Delta^{13}F_{\text{DIC}}} \times \frac{C_{\text{produced}}}{t} \quad (1)$$

With C_{produced} representing the concentration of the C pool or PLFA (in mol L^{-1}); t was equal to the duration of the experiment, and the difference in the carbon isotopic fractions (F) between sample and background ($\Delta^{13}\text{F}$) is

$$\Delta^{13}\text{F} = {}^{13}\text{F}_{\text{sample}} - {}^{13}\text{F}_{\text{background}} \quad (2)$$

following Middelburg (2014), where ${}^{13}\text{F}_{\text{background}}$ is the natural abundance ratio as measured before label addition (T_0), and ${}^{13}\text{F}_{\text{sample}}$ the ratio after the experiment (T_4) and with ${}^{13}\text{F}$ representing the fraction ${}^{13}\text{C}$, calculated as:

$$\frac{{}^{13}\text{C}}{{}^{12}\text{C} + {}^{13}\text{C}} = \frac{R}{R + 1} \quad (3)$$

R, the isotope ratios were derived from $\delta^{13}\text{C}$ values as

$$R = [(\delta^{13}\text{C}/1000) + 1] \times R_{\text{VPDB}} \quad (4)$$

using $R_{\text{VPDB}} = 0.0111796$ (Coplen 2011) and $\delta^{13}\text{C}$ being defined as the ratio of ${}^{13}\text{C}$ to ${}^{12}\text{C}$ as measured in a sample relative to the same ratio measured in a standard (in this case VPDB). Compound specific enrichment ($\Delta\delta^{13}\text{C}$, Middelburg 2014) values $> 1.5\text{‰}$ were used in calculations, with

$$\Delta\delta^{13}\text{C} = \delta^{13}\text{C}_{\text{sample}} - \delta^{13}\text{C}_{\text{background}} \quad (5)$$

Only for the bicarbonate-labelled incubations using $\Delta^{13}\text{F}_{\text{DIC}}$ is necessary as for glucose-labelled incubations we assume the DOC-pool to be completely labelled. Glucose is likely more easily consumed than naturally available, more refractory DOC pool.

Net primary production (NPP rate) was calculated from the sum of label that was transferred to POC and DOC in bicarbonate-labelled incubations (light conditions), while label transfer to POC in glucose-labelled incubations under dark conditions represented glucose-based production by bacteria (GBP, or heterotrophic bacterial production). The 2011 bottle-incubations allow calculating rates of NPP, GBP and respiration. For these calculations, steady-state was assumed, which considering the duration of the experiment and the absence of systematic changes in concentrations of carbon pools seems reasonable. Respiration was calculated from label transfer to DIC in the dark incubations. From the glucose-labelled incubations, bacterial growth efficiency (BGE) was calculated as

$$\text{BGE} = \frac{[\text{POC}]_{\text{labelled}}}{[\text{POC} + \text{DIC}]_{\text{labelled}}} \quad (6)$$

Hence both BGE and GBP are based on the dark incubations, using labeled glucose. To calculate the

isotopic composition of the respired carbon at natural abundance, a linear trend line was fitted to a Keeling-plot ($1/[DIC]$ vs. $\delta^{13}C_{DIC}$ at T_0 for each depth) using background DIC isotope values.

Results

Bottle labelling experiments

Physical and chemical parameters

A temperature profile of Lake Lucerne is shown in Fig. 2a, indicating that the thermocline during the 2012 experiment began at ~ 3 m depth, with temperatures decreasing strongly from 18 to 13 °C between 3 and 5 m. Below 5 m temperatures decreased more gradually, reaching stable values around 5 °C from 30 m depth downwards. Concentrations of dissolved oxygen (Fig. 2b) were around $370 \mu\text{mol L}^{-1}$ in the top 3 m, increasing in the thermocline to a maximum of $460 \mu\text{mol L}^{-1}$ at 10 m water depth. Oxygen concentrations decreased again below 10 m, reaching relatively stable concentrations below 30 m between 350 and $380 \mu\text{mol L}^{-1}$. The 100% saturation line of dissolved oxygen is shown as a grey line in Fig. 2b and indicates supersaturation in surface waters and undersaturation below 30 m water depth. Alkalinity (Fig. 2c) values decreased from 1.98 mM to 1.94 mM between 5 and 10 m depth, below which alkalinity gradually increased, reaching a maximum of 2.07 mM at 75 m depth.

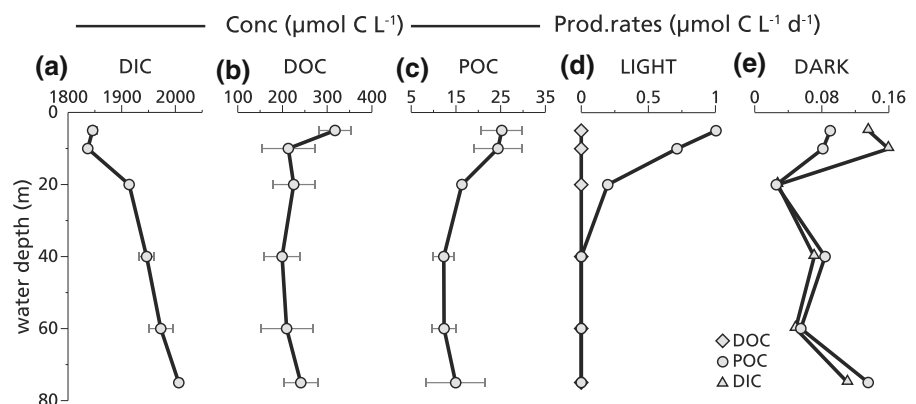
Carbon pools

Average DIC concentrations (Fig. 4a) were 1850 and $1840 \mu\text{mol L}^{-1}$ at 5 and 10 m respectively, increasing sharply to $1910 \mu\text{mol L}^{-1}$ at 20 m and then gradually increasing to $2010 \mu\text{mol L}^{-1}$ at 75 m depth. Average DOC concentrations (Fig. 4b) decreased from 320 to $210 \mu\text{mol L}^{-1}$ between 5 and 10 m depth, below which they remained stable throughout the water column. At 5 and 10 m, average POC concentrations (Fig. 4c) were relatively stable, with values of 25 and $24 \mu\text{mol L}^{-1}$ respectively, decreasing sharply to $16 \mu\text{mol L}^{-1}$ at 20 m. At greater water depths POC concentrations remained relatively stable around $12 \mu\text{mol L}^{-1}$. Because of the different initial carbon concentrations of the different carbon pools, the impact of labeling differed and we calculated effect of the isotopic label added accordingly.

Since the same amount of ^{13}C -bicarbonate was added at each depth, but initial DIC concentrations varied, the $\delta^{13}\text{C}$ of DIC after tracer addition increased by 114–127‰, with a larger increase corresponding to lower initial DIC concentrations. Transfer of label from DIC to DOC (Fig. 4d) was negligible during the incubations under light conditions. Label incorporation into POC (Fig. 4d) was highest at 5 m with values of $1.0 \mu\text{mol C L}^{-1} \text{ day}^{-1}$, decreasing to below detection at 40 m depth. A ^{13}C mass balance for organic and inorganic carbon pools was achieved within 18%, which is acceptable for our purposes.

Similar to bicarbonate labelling, the same amount of ^{13}C -glucose was added to each depth for dark incubations, while initial DOC concentrations varied. The different initial DOC concentrations resulted in stable carbon isotopic enrichment of the DOC varying

Fig. 4 Average concentrations for the bottle experiments (T_0 and light and dark incubations) of **a** DIC, **b** DOC and **c** POC in $\mu\text{mol C L}^{-1}$. Production rates (absolute label incorporation per day) under **d** bicarbonate-labelled light conditions and **e** glucose-labelled dark conditions in $\mu\text{mol C L}^{-1} \text{ day}^{-1}$



between 250 and 680‰, with the exception of 20 m depth, for which $\Delta\delta^{13}\text{C}$ values were 1250‰, likely resulting from the accidental double addition of label at the start of the experiment. Transfer of ^{13}C to DIC in dark incubations (Fig. 4e) was 0.14 and 0.16 $\mu\text{mol C L}^{-1} \text{ day}^{-1}$ at 5 and 10 m, decreasing to relatively low values around 0.03 $\mu\text{mol C L}^{-1} \text{ day}^{-1}$ at greater depth, with the exception of 40 and 75 m, where production rates reached higher values of 0.07 and 0.11 $\mu\text{mol C L}^{-1} \text{ day}^{-1}$ respectively. Label transfer to POC (Fig. 4e) showed a similar trend, except that values were somewhat lower at the surface (0.09 and 0.08 $\mu\text{mol C L}^{-1} \text{ day}^{-1}$ at 5 and 10 m depth respectively) and somewhat higher below 20 m. Excluding 20 m depth, a ^{13}C mass balance for organic and inorganic carbon pools was achieved within 15%.

Production and respiration

Since no appreciable transfer of ^{13}C to DOC was observed under light conditions (Fig. 4e), NPP is based solely on label incorporation into POC. Heterotrophic production rates (Table 1, calculated as label transfer to POC in glucose-labelled incubations) were positive at all depths, albeit much lower than NPP rates. Glucose-based heterotrophic production rates at 5, 10 and 40 m were similar, ranging between 0.08 and 0.09 $\mu\text{mol C L}^{-1} \text{ day}^{-1}$, while relatively low rates of 0.03 and 0.05 $\mu\text{mol C L}^{-1} \text{ day}^{-1}$ were observed at 20 m and 60 m depth. Maximum rates of 0.14 $\mu\text{mol C L}^{-1} \text{ day}^{-1}$ were reached at 75 m water depth.

Using the transfer of label to DIC in dark incubations, respiration rates (Table 1) were calculated,

which follow the same trend with depth as glucose-based production rates, with the exception that respiration rates were higher at 5 and 10 m, and lower below 20 m depth. By plotting natural abundance (T_0) samples in a Keeling-plot (not shown), it was derived that the $\delta^{13}\text{C}$ of respired DIC was -31.4‰ . Bacterial growth efficiency (BGE, Table 1) decreased from 0.40 to 0.34 between 5 and 10 m. Below 10 m it increased with depth to a maximum value of 0.55 at the deepest incubation depth of 75 m.

PLFA concentrations and label uptake

The main labelled PLFAs in the bicarbonate-labelled incubations during the 2011 bottle experiment were C16:2 ω 7, C16:3 ω 3, C16:3 ω 4, C16:4 ω 1, C18:3 ω 6, C18:3 ω 3 (α -linolenic acid, or ALA), C18:4 ω 3 (stearidonic acid, or SDA), C20:5 ω 3 (eicosapentaenoic acid, or EPA) and C20:4 ω 6 (arachidonic acid, or ARA). These PLFAs are produced by a variety of phytoplankton groups (e.g. Bacillariophyceae, Haptophytes, Chlorophytes, Chrysophytes, Cryptophytes, and also cyanobacteria) (Gugger et al. 2002; Dijkman and Kromkamp 2006; Taipale et al. 2013), but based on incorporation of labelled bicarbonate compared to glucose, these PLFAs were split into two groups (autotroph and mixotroph). PLFAs C16:3 ω 3, C18:3 ω 6, C18:3 ω 3, C18:4 ω 3 and C20:4 ω 6 showed minor (2–3 orders of magnitude less) incorporation of glucose compared to bicarbonate. Accordingly, they are combined to represent (photo)autotrophic producers. Glucose-derived label incorporation was higher for PLFAs C16:2 ω 7, C16:3 ω 4, C16:4 ω 1 and

Table 1 Net primary production (NPP), glucose-based heterotrophic production (GP) and respiration (R) in $\mu\text{mol C L}^{-1} \text{ day}^{-1}$ and bacterial growth efficiency (BGE) with depth

Water depth (m)	NPP ($\mu\text{mol C L}^{-1} \text{ day}^{-1}$)	GP	R	BGE
5	1.00	0.09	0.14	0.40
10	0.71	0.08	0.16	0.34
20	0.20	0.03	0.03	0.48
40	0.00	0.08	0.07	0.54
60	0.00	0.05	0.05	0.53
75	0.00	0.14	0.11	0.55
Depth integrated ($\text{mmol C m}^{-2} \text{ day}^{-1}$)	15.8	7.8	7.7	

Depth integrated primary production, glucose-based production and respiration rates in $\text{mmol C m}^{-2} \text{ day}^{-1}$

C20:5 ω 3, and hence their weighted sum is used to represent mixotrophic phytoplankton.

In glucose-labelled dark incubations, heterotrophic production is represented by branched PLFAs iC14:0, i/aC15:0 and iC16:0, which derive primarily from gram-positive bacteria (Kaneda 1991), although they have also been found in gram-negative bacteria (Zelles 1999). Labelling of branched PLFAs observed in bicarbonate-labelled incubations derives indirectly from autotrophic production via consumption of photosynthetically produced organic matter or from production by chemoautotrophic bacteria. Monounsaturated fatty acid PLFA C16:1 ω 7c is a common PLFA in many organisms (including chemoautotroph and heterotroph producers) and should therefore normally not be used as a biomarker for a specific group. However, in labelling studies such as the bottle experiments, label transfer into PLFA C16:1 ω 7c is informative and can be interpreted when considering the labelled substrate, labelling conditions and environmental context. Enrichment of C16:1 ω 7c in dark glucose-labelled incubations derives from heterotrophic production, while in bicarbonate-labelled light incubations it derives from autotrophic production. In bicarbonate-labelled incubations at greater depth, where light penetration is not sufficient to sustain considerable photoautotrophic production, chemoautotrophic production is responsible for enrichment of C16:1 ω 7c. Nevertheless, for clarity C16:1 ω 7c is shown separately in figures and has not been included in the summed values for autotroph and heterotroph production (Fig. 5). Concentrations and production rates of PLFA C18:1 ω 7c, which can derive from both phytoplankton (Dijkman and Kromkamp 2006; Taipale et al. 2013) and bacteria (White et al. 1996), were similar to concentrations and production rates of heterotroph-derived branched PLFAs and will not be discussed separately.

Production rates in nmol C L⁻¹ day⁻¹ for incubations under light conditions are shown in Fig. 5a. Photoautotrophic production rates decreased from 0.9 nmol C L⁻¹ day⁻¹ at 5 m to below detection limit at 20 m and below. Mixotrophic production rates based on PLFAs showed the same trend but were somewhat lower (0.24 nmol C L⁻¹ day⁻¹ and 0.07 nmol C L⁻¹ day⁻¹ at 5 and 10 m respectively). Bacterial production rates were highest at 5 m depth with a value of 0.2 nmol C L⁻¹ day⁻¹, decreasing to below detection limit at 20 m and below, except for

60 m depth where production reached a rate of 0.01 nmol C L⁻¹ day⁻¹. The ratio of the weighted averages of bacterial versus phytoplankton specific enrichment ($\Delta\delta^{13}\text{C}_{\text{bact}}/\Delta\delta^{13}\text{C}_{\text{phyto}}$) was 0.28, indicating that 28% of the bacterial carbon was derived from newly fixed phytoplankton biomass. PLFA C16:1 ω 7c showed highest production rates in Lake Lucerne with values increasing from 1.4 nmol C L⁻¹ day⁻¹ at 5 m to 2.0 nmol C L⁻¹ day⁻¹ at 10 m, subsequently decreasing to below detection limit at 20 m and below, with the exception of 60 m depth, where a relatively low production rate of 0.08 nmol C L⁻¹ day⁻¹ was observed.

Production rates for glucose-labelled incubations under dark conditions (Fig. 5b) for autotrophic production are slightly above detection limit, reaching 0.001 nmol C L⁻¹ day⁻¹ at 5 m, decreasing to below detection limit at 40 m and below. Production of the mixotroph derived PLFAs increased from 0.006 to 0.01 nmol C L⁻¹ day⁻¹ between 5 and 10 m water depth, decreasing to below detection limit at 60 m and below. A maximum production rate for bacterial PLFAs of 0.06 nmol C L⁻¹ day⁻¹ was observed at 5 m depth, decreasing to 0.01 nmol C L⁻¹ day⁻¹ at 40 m depth and then increasing again to 0.04 nmol C L⁻¹ day⁻¹ at 75 m water depth. PLFA C16:1 ω 7c showed the highest glucose-based production rates in Lake Lucerne with values reaching 0.22 nmol C L⁻¹ day⁻¹ at 5 m, decreasing to values between 0.02 and 0.05 nmol C L⁻¹ day⁻¹ between 20 and 60 m depth. A maximum value of 0.27 nmol C L⁻¹ day⁻¹ was observed at 75 m, about 5 m above the sediment–water interface.

Photoautotrophic phytoplankton derived PLFAs showed a maximum concentration of 4.0 \pm 1.0 nmol L⁻¹ at 5 m, decreasing to 1.3 \pm 0.1 nmol L⁻¹ at 20 m, below which values were close to zero, ranging between 0.8 \pm 0.2 and 0.3 \pm 0 nmol L⁻¹ (Fig. 5c). Mixotrophic phytoplankton derived PLFA concentrations were highest at the top of the water column with a value of 4.5 \pm 0.7 nmol L⁻¹ at 5 m, decreasing to 0.8 \pm 0.4 nmol L⁻¹ at 60 m. Between 60 and 75 m, concentrations increased to 3.2 \pm 0 nmol L⁻¹. Bacterial derived PLFA concentrations showed a decrease from 5.6 \pm 0.9 to 0.9 \pm 0.1 nmol L⁻¹ between 5 and 60 m depth, below which concentrations increased to 2.1 \pm 0.9 nmol L⁻¹ at 75 m depth. Concentrations of PLFA C16:1 ω 7c increased from 21.8 \pm 6.9 to 24.7 \pm 15.5 nmol L⁻¹ between 5 and 10 m depth,

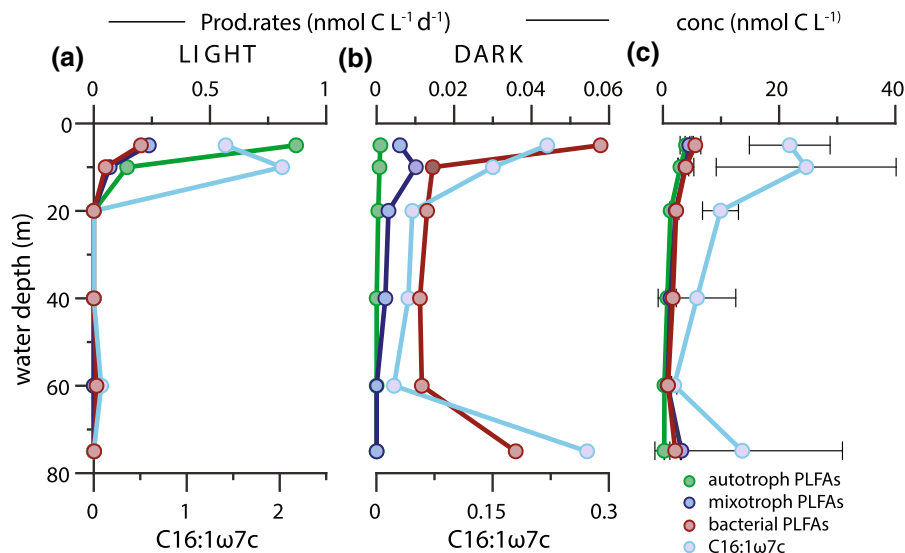


Fig. 5 Bottle experiment base production rates in **a** light and **b** dark incubations are plotted in $\text{nmol C L}^{-1} \text{ day}^{-1}$, **c** PLFA concentrations (\pm SD) as averages of T₀, T₄ light and T₄ dark in nmol C L^{-1} . Autotrophs shown in green are represented by PLFA C16:3 ω 3, C18:3 ω 6, C18:3 ω 3, C18:4 ω 3 and C20:4 ω 6.

Mixotrophs (blue) are PLFA C16:2 ω 7, C16:3 ω 4, C16:4 ω 1 and C20:5 ω 3. Bacteria (red) are represented by PLFA iC14:0, iC15:0, aC15:0 and iC16:0. PLFA C16:1 ω 7c, which can derive from different producers (see Sect. 3.1.4) is plotted in purple

decreasing to $1.9 \pm 0.4 \text{ nmol L}^{-1}$ at 60 m. A higher concentration of $13.6 \pm 17.2 \text{ nmol L}^{-1}$ was observed at the maximum incubation depth of 75 m.

Mesocosm labelling experiment

Physical and chemical parameters

Water temperatures (Fig. 6a) steadily increased over the duration of the experiment from $6.7 \text{ }^\circ\text{C}$ at T₀ to $9.8 \text{ }^\circ\text{C}$ at T₁₄. Dissolved oxygen concentrations are shown in Fig. 6b and were high and relatively stable, ranging between 440 and $476 \text{ } \mu\text{mol L}^{-1}$, although values at T₇ were even higher at $512 \text{ } \mu\text{mol L}^{-1}$. Alkalinity (Fig. 6c) somewhat increased during the experiment from 2.08 mM at T₀ to 2.14 mM at T₇, subsequently decreasing again to 2.08 mM at T₁₄.

The carbon isotopic composition of DIC before label addition (T₀) was -7.1‰ (Fig. 6d). The ^{13}C -bicarbonate addition resulted in constant-labelling with the $\delta^{13}\text{C}$ of DIC increasing to 441‰ at T₁, and stabilizing around 370‰ from T₂ until the end of the experiment.

Light penetration was somewhat reduced inside the mesocosm because of the material used, with Secchi depths ranging between 2.5 and 5 m, in contrast to the

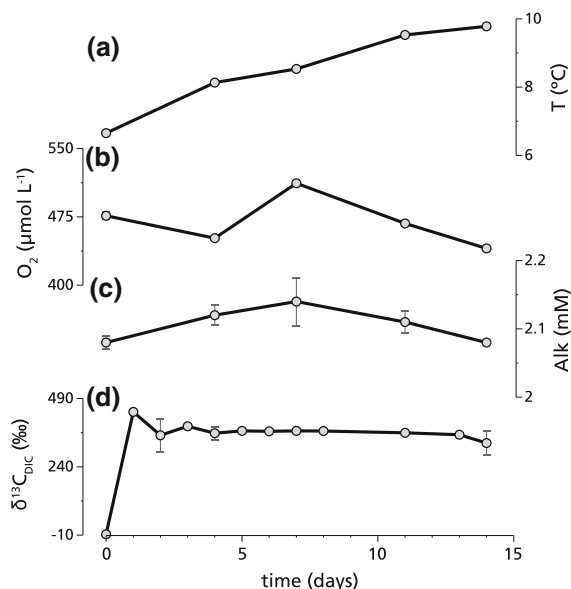


Fig. 6 Physical parameters during the 2012 mesocosm experiment. From top to bottom: **a** water temperature in $^\circ\text{C}$; **b** dissolved oxygen concentrations in $\mu\text{mol L}^{-1}$; **c** alkalinity in mM; **d** Carbon isotopic composition of DIC in ‰ versus VPDB

9–11 m depth outside the mesocosm. Productivity in the mesocosm may have been hindered by this, but water within the mesocosm was well-mixed, at least during the first stages of the experiment, and

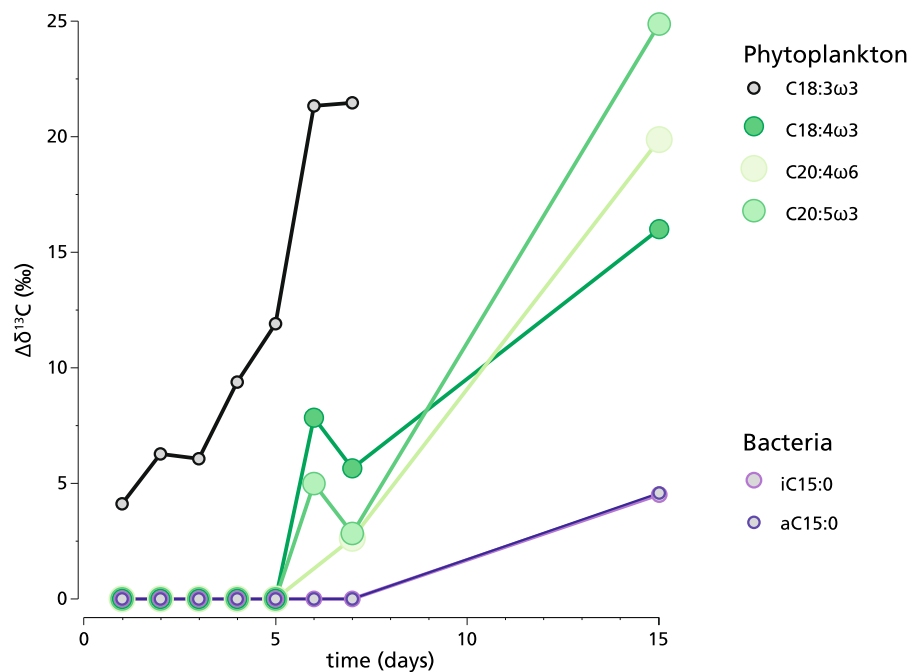
phytoplankton was thus intermittently exposed to sufficient light.

PLFA concentrations and label uptake

After the mesocosm labelling experiment only a limited number of PLFAs showed isotopic enrichment values $> 1.5\text{‰}$: branched PLFAs *i*C15:0 and *a*C15:0 and also phytoplankton-derived PLFAs C18:3 ω 3, C18:4 ω 3, C20:4 ω 6 and C20:5 ω 3. Stable carbon isotope values of the phytoplankton PLFAs showed that label incorporation took place at different rates: early (within 1 day) and with a time lag (from day 6) (Fig. 7). PLFA C18:3 ω 3 showed label incorporation first and is therefore used to represent early-growing phytoplankton. In contrast, the sum of PLFA C18:4 ω 3, C20:4 ω 6 and C20:5 ω 3 is used to calculate enrichment and production rates of the late-growing phytoplankton. Based on relative label uptake, these PLFAs were produced both autotrophically (C18:4 ω 3 and C20:4 ω 6) and mixotrophically (C20:5 ω 3) during the bottle experiments. Weighted averages of branched PLFA *i*C15:0 and *a*C15:0 are used to represent heterotrophic bacteria (hereafter heterotrophs) (see above).

Relative label incorporation expressed as $\Delta\delta^{13}\text{C}$ (specific enrichment) for PLFAs is shown in Fig. 7 and shows that enrichment was not only fastest, but also highest for PLFA C18:3 ω 3, with a 4.1‰ enrichment at T_1 , increasing to a $\Delta\delta^{13}\text{C}$ of 21.5‰ at T_7 . Unfortunately, peak separation for C18:3 ω 3 in the T_{15} sample was poor, and low concentrations did not allow for duplicate analyses, preventing calculation of a proper $\Delta\delta^{13}\text{C}$ value. Relative enrichment of late-growing PLFAs shows $\Delta\delta^{13}\text{C}$ values at or close to zero until T_5 . After T_5 , PLFA enrichment increased strongly with the exception of a 2‰ decrease at T_7 . Final enrichment values at T_{15} varied between 16 and 25‰. Concentrations of C18:3 ω 6 (γ -linolenic acid or GLA), which can be used to represent cyanobacteria (Gugger et al. 2002; De Kluijver et al. 2012) were very low or not present. This indicates that they are either minor producers in Lake Lucerne during this period, or that the cyanobacterial community consists of species that do not produce this specific PLFA. Bacterial PLFAs (Fig. 7, purple shades) were not labelled considerably until after day seven, subsequently reaching a maximum $\Delta\delta^{13}\text{C}$ of 4.6‰ at T_{15} . The ratio of the weighted averages of the bacterial versus phytoplankton specific enrichments ($\Delta\delta^{13}\text{C}_{\text{bact}}/\Delta\delta^{13}\text{C}_{\text{phyto}}$) was 0.22, indicating that 22% of the bacterial

Fig. 7 Relative label incorporation into biomarker PLFA expressed as $\Delta\delta^{13}\text{C}$ in ‰ versus VPDB. Phytoplankton-derived PLFA are shown in black and green shades. Bacterial PLFA are plotted in shades of purple



carbon was derived from newly fixed phytoplankton biomass at the end of the experiment.

Production rates in $\text{nmol C L}^{-1} \text{ day}^{-1}$ for PLFAs grouped as early-/late-growing phytoplankton and heterotrophic bacteria are given in Table 2. For early-growing phytoplankton, production rates based on ^{13}C -labelling were observed from day 1 ranging between 0.007 and 0.014 $\text{nmol C L}^{-1} \text{ day}^{-1}$ with a mean of 0.011 $\text{nmol C L}^{-1} \text{ day}^{-1}$. For late-growing phytoplankton production rates were below detection limit until T_5 , then ranging between 0.005 and 0.009 $\text{nmol C L}^{-1} \text{ day}^{-1}$, with a mean of 0.007 $\text{nmol C L}^{-1} \text{ day}^{-1}$. Heterotroph production rates were undetectable until T_{15} , reaching 0.002 $\text{nmol C L}^{-1} \text{ day}^{-1}$.

Discussion

Depth-profile of carbon flows

In this study, net primary production (NPP) is based on label incorporation into POC in light incubations, which partly might be transferred to the DOC pool. In Lake Lucerne, however, no substantial transfer to the DOC pool was observed over the duration of the experiment and hence NPP is solely based on production of POC (Fig. 4d, Table 1). NPP showed a clear decrease with depth, with a maximum rate of 1 $\mu\text{mol C L}^{-1} \text{ day}^{-1}$ at 5 m and a low production rate of 0.2 $\mu\text{mol C L}^{-1} \text{ day}^{-1}$ at 20 m water depth. Below 20 m, no substantial labelling of POC ($> 5\%$) was observed, indicating that NPP at those depths is insignificant. This is consistent with summer Secchi depths of about 5.8 ± 1.4 m in Lake Lucerne (Bos-sard et al. 2001).

To quantify bacterial production and respiration, labelled glucose was added as a substrate. Compared to the naturally available DOC, glucose is likely degraded more easily and hence the glucose-based production and respiration rates used here are likely overestimates, representing potential rates. Conversely, production and respiration by some microbes that do not use glucose could not be traced. During the bottle experiments, GBP values were low (around 0.08 $\mu\text{mol C L}^{-1} \text{ day}^{-1}$, Fig. 4e, Table 1) and relatively stable throughout the water column with only somewhat higher rates observed near the surface and deeper in the water column. GBP at 5 and 10 m water depth is likely related to photoautotrophic production since heterotrophic activities are positively correlated with primary production (Cole et al. 1988). This is confirmed by the ^{13}C light incubations, showing transfer of ^{13}C -DIC via phytoplankton to heterotrophic bacteria (Fig. 5a). At 75 m water depth, near the lake floor, a higher GBP may derive from slowly settling or re-suspended material, since no local primary production was observed (Fig. 4d). A higher GBP rate may also be inferred at 40 m, although there was no evidence for increased supply of substrate to explain higher rates of GBP and differences are small. Since the low POC concentrations did not allow for true replication it is difficult to quantify error propagation and we therefore refrain from explaining such minor features.

The relative rates of NPP and respiration provide crucial information about the potential for storage or release of carbon from the lake system. In many unproductive systems, respiration is higher than NPP, indicating that microbes must consume external (allochthonous) organic matter, resulting in higher lake pCO_2 and a subsequent net flux of CO_2 into the atmosphere (Del Giorgio and Peters 1994; Del Giorgio

Table 2 Minimum, maximum and average production rates as measured during the mesocosm experiment in $\text{nmol C L}^{-1} \text{ day}^{-1}$ for phytoplankton and heterotrophic bacteria

	Early-growing phytoplankton	Late-growing phytoplankton	Heterotroph
Min ($\text{nmol C L}^{-1} \text{ day}^{-1}$)	0.007	0.005	
Max ($\text{nmol C L}^{-1} \text{ day}^{-1}$)	0.014	0.009	
Mean ($\text{nmol C L}^{-1} \text{ day}^{-1}$)	0.011	0.007	0.002
Turnover (days)	130	560	3670

The slow label transfer to heterotrophs did not allow for the calculation of minimum or maximum production rates

et al. 1997). Integrated over the water column, respiration rates were approximately 50% lower than rates for NPP, indicating Lake Lucerne was net autotrophic during our experiment (Table 1). Still, it should be noted that the experiment took place during the most productive season of the year.

Transfer of ^{13}C -glucose to DIC exceeds that to POC near the surface, showing that glucose-catabolism is more important than glucose-anabolism, possibly as a result of competition for nutrients with phytoplankton (Bratbak and Thingstad 1985; Litchman et al. 2004), although there may also be other factors influencing the partitioning of carbon (e.g., del Giorgio and Cole 1998). The strong coupling between DIC and POC labeling below 10 m water depth suggests growth of heterotrophic producers is not nutrient limited deeper in the water column, which is in line with earlier observations (Bossard et al. 2001). Relative rates of GBP and respiration can be expressed in bacterial growth efficiencies (BGE, Table 1), which increase below 10 m water depth. Although reports are inconclusive whether glucose-addition stimulates growth under oligotrophic conditions (Del Giorgio and Cole 1998), this seems likely in our experiment since BGE's in oligotrophic systems are usually much lower than those observed here. More complex substrates that make up most of the natural DOC-pool are likely more refractory and hence extrapolation from a single compound such as glucose may lead to overestimation of BGEs ((Del Giorgio and Cole 1998) and references therein).

Phytoplankton production

Photoautotrophy

Autotroph-derived PLFAs in bicarbonate-labelled light incubations (Fig. 5a) show decreasing photosynthetic production rates with depth. Maximum oxygen concentrations at 10 m depth exceeded maximum solubility of oxygen at the in situ temperatures (Fig. 2b), which is in line with the observed highest NPP at this depth. Below this depth productivity is much lower, decreasing to a production rate of $0.2 \mu\text{mol L}^{-1} \text{day}^{-1}$ at 20 m water depth. The lack of substantial label uptake in some of the individual PLFAs at this depth, with production ongoing, indicates that photosynthesis did not result in biomass addition, but rather resulted in enhanced storage of

carbohydrates (sugars) as a result of nutrient and/or light depletion (Granum et al. 2002; Grosse et al. 2015). Also in the dark experiments low production rates for autotroph-derived PLFAs were observed, albeit that these rates are two to three orders of magnitude lower compared to bicarbonate-based production at the corresponding depths (Fig. 5b).

Chemoautotrophy

Carbon fixation by bacteria or archaea using energy obtained from inorganic electron donors rather than sunlight is called chemo-litho-autotrophy. In the DIC-labelled incubations the isotopic signatures of branched bacterial PLFAs and the more general PLFA C16:1 ω 7c showed some isotopic enrichment at 60 m water depth, indicating this was probably the main depth for chemoautotrophic production, which is in line with Blaga et al. (2011). Blaga et al. (2010) showed highest chemoautotrophic production taking place below 40 meters water depth. Production rates are, however, low compared to photosynthetic production in the top 10 m of the water column and only the branched and general PLFA C16:1 ω 7c were labelled. Consequently, chemoautotrophic production rates contribute little to primary production in Lake Lucerne.

Mixotrophy

The ability of certain phytoplankton species to switch between inorganic and organic carbon sources for the production of biomass is called mixotrophy. For some organisms, such as diatoms amongst others, it is known that they are able to take up carbohydrates to metabolize (Lewin 1953). Mixotroph-derived PLFAs observed in this study (C16:2 ω 7, C16:3 ω 4, C16:4 ω 1 and C20:5 ω 3) can be produced by Bacillariophyceae (diatoms), although C20:5 ω 3 is also produced by Rhodophyta, Cryptophyta and Haptophyta (Dijkman and Kromkamp 2006). Mixotrophic production was substantial in the bottle experiments (Fig. 5a, b), with production rates (summed production based on bicarbonate and glucose) at 5 and 10 m of 28 and 55% of phototrophic production rates respectively. At 5 m water depth, DIC was more important as a substrate for the production of these PLFAs, whereas at 10 m depth production rates in light (DIC) and dark (DOC) incubations were of the same order of magnitude.

More similar production rates for autotrophs and mixotrophs at 10 m depth compared to 5 m indicate that mixotrophy is a metabolic advantage for mixotrophs to keep up production at this depth, where light availability limits phototrophic growth.

Bacterial production

Glucose incorporation into bacterial branched PLFAs and PLFA C16:1 ω 7c in the dark incubations derives from heterotrophic production (Fig. 5b). It should be noted that PLFA C16:1 ω 7c is produced by both bacteria and phytoplankton and hence in the dark bottle incubations at 5 and 10 m water depth may partly derive from mixotrophs, which showed substantial growth at these depths. Diatoms, as potential mixotrophic producers at these depths (see above) produce lower amounts of C16:1 ω 7c compared to the studied mixotroph PLFAs (Dijkman and Kromkamp 2006), yet the observed production rates of C16:1 ω 7c are much higher and show a different trend with depth. Differing trends and contrasting concentrations make it unlikely that production by mixotrophs substantially contributed to the labelling of C16:1 ω 7c in dark incubations. In general the pattern in C16:1 ω 7c corresponds well with the bacterial derived branched PLFAs and the GBP based on the dark incubations. Only at 10 m water depth, branched bacterial PLFAs and C16:1 ω 7c likely derived from different source organisms, since the production rate of production of C16:1 ω 7c was still high, while branched PLFA production decreased substantially.

Production of labelled branched bacterial PLFAs at 5 and 10 m water depth in the light incubations most likely derived from organic carbon exudation by phytoplankton: the release of excess organic molecules when carbon fixation was higher than incorporation into new cell material (Fogg 1983). Because of the labeled DIC being used by the phytoplankton exudated DOC became somewhat labeled as well. Although exudation of organic carbon by phytoplankton was not sufficient to change the carbon isotopic composition of the DOC pool (Fig. 4d), it is likely that some labelled organic carbon was produced nonetheless and preferentially used as a substrate by bacteria, since consumption of the extracellular compounds by heterotrophs was previously found to be both substantial and rapid (Fogg 1983). Moreover, rapid uptake of

exudates would actually counteract the transfer of label to the DOC pool (Morana et al. 2014).

From 5 to 10 m water depth a decrease in alkalinity was observed (Fig. 2c), which can result from different processes. Biological precipitation of CaCO₃ by calcifying organisms leads to a decrease in alkalinity (Zeebe and Wolf-Gladrow 2001) and also primary production based on ammonium (Soetaert et al. 2007), and oxidation of reduced nitrogen (nitrification) and sulfur, generated during remineralization of algae, will decrease alkalinity (Wolf-Gladrow et al. 2007). In Lake Lucerne remineralization is a possible explanation for the lower alkalinity values at 10 m depth, since it is in line with the observed maximum in glucose-based respiration rates at this depth. Moreover, at 10 m water depth, a maximum can be observed in bicarbonate-based production of C16:1 ω 7c, which is produced by many organisms including nitrifying bacteria (Guezennec and Fialamedioni 1996; Lipski et al. 2001; de Bie et al. 2002) and sulfur-oxidizing bacteria (Zhang et al. 2005; van Gaever et al. 2009). In Lake Lucerne, a maximum in calcite precipitation caused by picocyanobacteria was previously identified at 10 m water depth during summer. The PLFA concentration profiles showed no indication for higher cyanobacterial abundance at 10 m although cyanobacterial production cannot be ruled out, since not all cyanobacteria produce unique PLFAs.

Comparison to eutrophic Lake Rotsee

A second bottle labelling experiments similar to the one in Lake Lucerne was carried out in Rotsee during the same month (Lammers et al. 2016). Rotsee is a eutrophic lake north of Lake Lucerne (Fig. 1), which is connected to Lake Lucerne via the Reuss-Rotsee canal. Because of their proximity, surface light conditions, air temperatures and precipitation in winter and spring before the experiments were very similar. Hence, differences in the carbon fluxes between Lake Lucerne and Rotsee result from their contrasting trophic states and corresponding microbial communities.

The depth-integrated NPP rate was ~ 24 times higher in eutrophic Rotsee compared to oligotrophic Lake Lucerne. The much deeper photic zone in oligotrophic Lake Lucerne apparently does not compensate for the much higher volumetric NPP rates in

Rotsee. However, rates of glucose-based production and respiration were only 3.5 and 4.5 times higher in Rotsee respectively. This indicates a closer coupling of respiration with NPP in Lake Lucerne, which is expected since availability of substrates is limited in oligotrophic Lake Lucerne. Overall, in Lake Lucerne the sum of glucose-based production and respiration rates are approximately equal to the rate of NPP. Efficient respiration is also reflected by the sedimentary C_{org} content, which is relatively low at 1.5–3% (Blaga et al. 2011). In Rotsee, the much higher NPP rate compared to the sum of glucose-based production and respiration rates potentially results in net carbon storage in the sediment, in line with a C_{org} content of 10–11% (data not shown).

Mesocosm labelling: carbon transfer to bacteria

Mesocosm conditions

During the mesocosm labelling experiment in spring, water temperatures rapidly increased by about 3 degrees in 14 days (Fig. 6a). From T_{11} , a thermocline starts to develop around 5 m water depth, with deeper water not warming to temperatures > 7.5 °C (data not shown). Surface water temperatures, however, were about 7.5 degrees colder in comparison to the bottle incubations in June (Fig. 2a), allowing for higher dissolved oxygen concentrations. At the observed temperatures between 6 and 10 °C, dissolved oxygen saturation concentrations range between ~ 400 and $353 \mu\text{mol L}^{-1}$ respectively. Higher observed oxygen concentrations between 440 and $510 \mu\text{mol L}^{-1}$ (Fig. 6b) indicate biological production of oxygen. Decreasing oxygen concentrations follow increasing water temperatures from T_7 onward, but do not explain the observed variability in oxygen concentrations before T_7 .

PLFA production

Production rates during the mesocosm experiment were relatively low for both phytoplankton and bacteria. The difference between calculated production in the mesocosm and the integrated bottle experiments is, however, in line with the timing during the year of the experiments. The observed rapid increase in water temperatures during the mesocosm experiment usually precedes the onset of the so-called

spring bloom. Additionally, the difference in bacterial production rates may partly be related to the so-called bottle-effect, with enhanced substrate-availability for heterotrophs in the bottle incubations stimulating productivity. However, there were also substantial differences between the experiments in terms of light climate, temperatures and turbulence. We are aware of the mysterious and somewhat controversial nature of the bottle-effect ((Hammes et al. 2010) and references therein), and the inherent difficulty to quantify this effect, refraining from further discussing it. Moreover, it should be noted that the lower values ($< 5\%$) of relative label incorporation during the mesocosm are close to the detection limit of the method, bringing uncertainty to the calculated production rate for heterotrophic bacteria. Also, the stratification in the mesocosm experiment during the later stage of the experiment might have affected integrated productivity by limiting productivity deeper in the mesocosm. Despite all these complicating factors, these experiments still capture the temporal evolution of the phytoplankton community and the role of this community in carbon cycling.

Production of phytoplankton PLFAs occurred at two different rates (Fig. 7, Table 2). The difference in isotopic enrichment and production rates of PLFA C18:3 ω 3 compared to C18:4 ω 3, C20:4 ω 6 and C20:5 ω 3 (Fig. 7) is suggestive of a change in the phytoplankton population as a result of changing conditions in the mesocosm.

In the mesocosm experiment in Lake Lucerne, transfer of newly fixed (labelled) carbon to bacteria lags behind early-growing phytoplankton more than 6 days and behind late-growing phytoplankton more than 2 days. A wide range in lag time has been observed in previous studies. De Kluijver et al. (2010) observed a lag of 2–3 days in incubations under different CO_2 levels. A lag of ~ 1 day was found in a mesocosm labelling study in a Danish estuary (Van den Meersche et al. 2004). Much longer lag times of 14 days (Hoppe et al. 2008) and ~ 1 month (Ducklow et al. 2001) have also been observed, likely related to colder (winter) temperatures. The relatively slow bacterial response during the Lucerne mesocosm experiment do not allow correlating phytoplankton dynamics with bacterial dynamics, or to determine whether bacteria had reached isotopic equilibrium during the 15-day experiment. Nevertheless, we calculate that only 22% of the bacterial carbon was

derived from recently fixed phytoplankton at the end of the experiment, which is consistent with the bottle experiments in which 28% of bacterial carbon was derived from labelled phytoplankton after the start of the experiment (4 days). In a whole-lake DIC ^{13}C -labelling experiment (56 days), an almost complete dependency (88–100%) of heterotrophic bacteria on autochthonous carbon was found (Pace et al. 2007). Mesocosm labelling experiments found bacterial dependency on recently fixed phytoplankton material as high as 70% (Lyche et al. 1996) and 87% (De Kluijver et al. 2010). Although it is questionable whether isotopic equilibrium was achieved in our experiment, the observed bacterial dependence seems to be relatively low, which, in combination with the observed time-lag shows uncoupling between phytoplankton and heterotrophic bacteria on the timescale of weeks.

Uncoupling of phytoplankton and bacteria can have several explanations, one being that it may take a while to produce labelled substrate available to heterotrophs. The transfer of carbon from phytoplankton to heterotrophs occurs mainly via the pool of labile dissolved organic matter (DOM), which becomes isotopically enriched through exudation of organic carbon. Since phytoplankton production rates were low it likely took some time to enrich the pool of labile DOM sufficiently to manifest itself in newly produced bacterial matter. A second explanation is a potential state of dormancy in bacteria when there is a lack of suitable energy-yielding substrates (Morita 1982). This is also in line with the faster labelling of bacterial biomass during the bottle experiment in early summer. Seasonal evolution in the occurrence and the length of lag periods has been demonstrated in seawater culture experiments (Ducklow et al. 1999). When there is strong coupling between phytoplankton and heterotrophic bacteria, degradation results in an almost instant remineralization of photosynthesized organic matter and in recycling of CO_2 . When there is a long time lag, dead phytoplankton biomass may sink and not be available for bacterial degradation in surface water, resulting in carbon export to deeper water.

Conclusions

The depth-integrated rate of NPP during the early summer bottle experiments in Lake Lucerne was

$15.8 \text{ mmol C m}^{-2} \text{ day}^{-1}$. During a similar experiment in nearby eutrophic Rotsee depth-integrated rates of NPP were ~ 24 times higher, showing that the deeper photic zone in Lake Lucerne didn't compensate for the higher volumetric NPP rates in Rotsee. In Lake Lucerne, autotrophic production was primarily located in the upper 20 m of the water column, but labelling of PLFAs provided evidence for some chemoautotrophic production at 60 m water depth. During the bottle experiments, label was transferred from phytoplankton to bacteria at 5 and 10 m depth and at the end of the experiment 28% of bacterial carbon was derived from freshly produced phytoplankton organic matter.

Depth-integrated glucose-based production and respiration rates were each $\sim 50\%$ of NPP rates (7.8 and $7.7 \text{ mmol C m}^{-2} \text{ day}^{-1}$ respectively). This close coupling between bacterial production and respiration with NPP was much stronger than in the Rotsee bottle experiments, where the depth-integrated NPP rate was > 12 times higher than the sum of glucose-based production and respiration (Lammers et al. 2016). This indicates that heterotrophic producers in Lake Lucerne are well adapted to rapidly respond to an increase in primary productivity, which is in line with calculated bacterial growth efficiencies in the surface water layer.

During the early spring mesocosm experiment, phytoplankton and bacterial production rates were 1–2 orders of magnitude lower than during the bottle experiments which coincided with a higher productivity period. Bacterial production showed a lag of about 6 days compared to early-growing phytoplankton. A small fraction of about 22% of the bacterial carbon was derived from phytoplankton production at the end of the experiment. Compared to the bottle experiment, coupling between phytoplankton and bacteria was weaker and potentially more organic matter could escape recycling. This uncoupling is likely related to slow transfer of phytoplankton organic carbon to the pool of labile DOM.

Acknowledgements The authors thank A.A. Scharfbillig, R.S. van den Broeke (Utrecht University) and M. Klockowski, G. Nobbe, M. Schurter and A. Zwyssig (EAWAG) for assistance during sampling. We also acknowledge M. Kienhuis, D. Kasjaniuk, A. van Leeuwen, A. van Dijk (UU) and M. Houtekamer and P. van Rijswijk (NIOZ Yerseke) for analytical support. The editor and 2 anonymous referees are thanked for constructive feedback. This research was funded by the Netherlands Organization for Scientific Research (NWO) under Grant Number 820.02.017. This work was carried out under the program of the Netherlands Earth System Science

Centre (NESSC), financially supported by the Dutch Ministry of Education, Culture and Science (OCW).

Open Access This article is distributed under the terms of the Creative Commons Attribution 4.0 International License (<http://creativecommons.org/licenses/by/4.0/>), which permits unrestricted use, distribution, and reproduction in any medium, provided you give appropriate credit to the original author(s) and the source, provide a link to the Creative Commons license, and indicate if changes were made.

References

- Battin TJ, Luysaert S, Kaplan LA, Aufdenkampe AK, Richter A, Tranvik LJ (2009) The boundless carbon cycle. *Nat Geosci* 2:598–600
- Blaga CI, Reichart G-J, Schouten S, Lotter AF, Werne JP, Kosten S, Mazzeo N, Lacerot G, Sinninghe Damste JS (2010) Branched glycerol dialkyl glycerol tetraethers in lake sediments: can they be used as temperature and pH proxies? *Org Geochem* 41:1225–1234
- Blaga CI, Reichart GJ, Vissers EA, Lotter AF, Anselmetti FS, Sinninghe Damsté JS (2011) Seasonal changes in glycerol dialkyl glycerol tetraether concentrations and fluxes in a perialpine lake: Implications for the use of the TEX₈₆ and BIT proxies. *Geochim Cosmochim Acta* 75:6416–6428
- Bloesch J, Stadelmann P, Buhner H (1977) Primary production, mineralization, and sedimentation in the euphotic zone of two Swiss Lakes. *Limnol Oceanogr* 22(3):511–526
- Boschker HTS, Moerdijk-Poortvliet TCW, van Breugel P, Houtekamer M, Middelburg JJ (2008) A versatile method for stable carbon isotope analysis of carbohydrates by high-performance liquid chromatography/isotope ratio mass spectrometry. *Rapid Commun Mass Spectrometry* 22:3902–3908
- Bossard P, Gammeter S, Lehmann C, Schanz F, Bachofen R, Bürgi HR, Steiner D, Zimmerman U (2001) Limnological description of the Lakes Zürich. *Lucerne Cadagno Aquat Sci* 63:225–249
- Bratbak G, Thingstad TF (1985) Phytoplankton-bacteria interactions: an apparent paradox? Analysis of a model system with both competition and commensalism. *Mar Ecol Prog Ser* 25:23–30
- Brett MT, Kainz MJ, Taipale SJ, Seshan H (2009) Phytoplankton, not allochthonous carbon, sustains herbivorous zooplankton production. *PNAS* 106(50):21197–21201
- Brett MT, Arhonditsis GB, Chandra S, Kainz MJ (2012) Mass flux calculations show strong allochthonous support of freshwater zooplankton production is unlikely. *PLoS ONE* 7(6):e39508
- Bürgi HR, Stadelmann P (2002) Alteration of phytoplankton structure in Lake Lucerne due to trophic conditions. *Aquat Ecosyst Health Manag* 5(1):45–59
- Bürgi HR, Heller C, Gaebel S, Mookerji N, Ward JV (1999) Strength of coupling between phyto- and zooplankton in Lake Lucerne (Switzerland) during phosphorus abatement subsequent to a weak eutrophication. *J Plankton Res* 21(3):485–507
- Buser HR, Arn H, Guerin P, Rauscher S (1983) Determination of double bond position in mono-unsaturated acetates by mass spectrometry of dimethyl disulfide adducts. *Anal Chem* 55(6):818–822
- Cole JJ, Findlay S, Pace ML (1988) Bacterial production in fresh and saltwater ecosystems: a cross-system overview. *Mar Ecol Prog Ser* 43:1–10
- Cole JJ, Prairie YT, Caraco NF, McDowell WH, Tranvik LJ, Striegl RG, Duarte CM, Kortelainen P, Downing JA, Middelburg JJ, Melack JM (2007) Plumbing the global carbon cycle: integrating inland waters into the terrestrial carbon budget. *Ecosystems* 10:171–184
- Cole JJ, Carpenter SR, Kitchell JF, Pace ML, Solomon CT, Weidel BC (2011) Strong evidence for terrestrial support of zooplankton in small lakes based on stable isotopes of carbon, nitrogen, and hydrogen. *PNAS* 108(5):1975–1980
- Coplen TB (2011) Guidelines and recommended terms for expression of stable-isotope-ratio and gas-ratio measurement results. *Rapid Commun Mass Spectrometry* 25:2538–2560
- de Bie MJM, Starink M, Boschker HTS, Peene JJ, Laanbroek HJ (2002) Nitrification in the Schelde estuary: methodological aspects and factors influencing its activity. *FEMS Microbiol Ecol* 42:99–107
- De Kluijver A, Soetaert K, Schulz KG, Riesebell U, Bellerby RGJ, Middelburg JJ (2010) Phytoplankton-bacteria coupling under elevated CO₂ levels: a stable isotope labelling study. *Biogeosciences* 7:3783–3797
- De Kluijver A, Yu J, Houtekamer M, Middelburg JJ, Liu Z (2012) Cyanobacteria as a carbon source for zooplankton in eutrophic Lake Taihu, China, measured by ¹³C labeling and fatty acid biomarkers. *Limnol Oceanogr* 57(4):1245–1254
- De Kluijver A, Soetaert K, Czerny J, Schulz KG, Boxhammer T, Riesebell U, Middelburg JJ (2013) A ¹³C labelling study on carbon fluxes in Arctic plankton communities under elevated CO₂ levels. *Biogeosciences* 10:1425–1440
- Del Giorgio PA, Cole JJ, Cimperlis A (1997) Respiration rates in bacteria exceed phytoplankton production in unproductive systems. *Nature* 385:148–151
- Del Giorgio PA, Cole JJ (1998) Bacterial growth efficiency in natural aquatic systems. *Annu Rev Ecol Syst* 29:503–541
- Del Giorgio PA, Peters RH (1994) Patterns in planktonic P: R ratios in lakes: influence of lake trophy and dissolved organic carbon. *Limnol Oceanogr* 39:772–787
- Dickson L, Bull ID, Gates PJ, Evershed RP (2009) A simple modification of a silicic acid lipid fractionation protocol to eliminate free fatty acids from glycolipid and phospholipid fractions. *J Microbiol Methods* 78:249–254
- Dijkman NA, Kromkamp JC (2006) Phospholipid-derived fatty acids as chemotaxonomic markers for phytoplankton: application for inferring phytoplankton composition. *Mar Ecol Prog Ser* 324:113–125
- Ducklow H, Carlson C, Smith W (1999) Bacterial growth in experimental plankton assemblages and seawater cultures from the *Phaeocystis antarctica* bloom in the Ross Sea, Antarctica. *Aquat Microbiol Ecol* 19(3):215–227
- Ducklow H, Carlson C, Church M, Kirchman D, Smith D, Steward G (2001) The seasonal development of the bacterioplankton bloom in the Ross Sea, Antarctica, 1994–1997. *Deep-Sea Res II* 48:4199–4221

- Fogg GE (1983) The ecological significance of extracellular products of phytoplankton photosynthesis. *Bot Mar* 26:3–14
- Granum E, Kirkvold S, Mykkestad SM (2002) Cellular and extracellular production of carbohydrates and amino acids by the marine diatom *Skeletonema costatum*: diel variations and effects of N depletion. *Mar Ecol Prog Ser* 242:83–94
- Grosse J, van Breugel P, Boschker HTS (2015) Tracing carbon fixation in phytoplankton—compound specific and total ^{13}C incorporation rates. *Limnol Oceanogr* 13:288–302
- Guezennec J, Fialamedioni A (1996) Bacterial abundance and diversity in the Barbados trench determined by phospholipid analysis. *FEMS Microbiol Ecol* 19:83–93
- Gugger M, Lyra C, Suominen I, Tsitko I, Humbert JF, Salkinoja-Salonen MS, Sivonen K (2002) Cellular fatty acids as chemotaxonomic markers of the genera *Anabaena*, *Aphanizomenon*, *Microcystis*, *Nostoc* and *Planktothrix* (cyanobacteria). *Int J Syst Evol Microbiol* 52:1007–1015
- Hammes F, Vital M, Egli T (2010) Critical evaluation of the volumetric “bottle effect” on microbial batch growth. *Appl Environ Microbiol* 76(4):1278–1281
- Heimann M (2009) Searching out the sinks. *Nat Geosci* 2:3–4
- Hoppe HG, Breithaupt P, Walther K, Koppe R, Bleck S, Sommer U, Jürgens K (2008) Climate warming in winter affects the coupling between phytoplankton and bacteria during the spring bloom: a mesocosm study. *Aquat Microb Ecol* 51:105–115
- Kaneda T (1991) Iso-fatty and anteiso-fatty acids in bacteria—biosynthesis, function and taxonomic significance. *Microbiol Rev* 55:288–302
- Lammers JM, Schubert CJ, Middelburg JJ, Reichart GJ (2016) Carbon flows in eutrophic Lake Rotse: a ^{13}C -labelling experiment. *Biogeochemistry* 131:147–162
- Lewin JC (1953) Heterotrophy in diatoms. *J Gen Microbiol* 9:305–313
- Lipski A, Spieck E, Makolla A, Altendorf K (2001) Fatty acid profiles of nitrite-oxidizing bacteria reflect their phylogenetic heterogeneity. *Syst Appl Microbiol* 24:377–384
- Litchman E, Klausmeier CA, Bossard P (2004) Phytoplankton nutrient competition under dynamic light regimes. *Limnol Oceanogr* 49:1457–1462
- Lyche A, Andersen T, Christoffersen K, Hessen DO, Hansen PHB, Klynsner A (1996) Mesocosm tracer studies. 2. The fate of primary production and the role of consumers in the pelagic carbon cycle of a mesotrophic lake. *Limnol Oceanogr* 41(3):475–487
- Middelburg JJ (2014) Stable isotopes dissect aquatic food webs from the top to the bottom. *Biogeosciences* 11:2357–2371
- Middelburg JJ, Barranguet C, Boschker HTS, Herman PMJ, Moens T, Heip CH (2000) The fate of intertidal microphytobenthos carbon: An in situ ^{13}C -labeling study. *Limnol Oceanogr* 45(6):1224–1234
- Morana C, Sarmiento H, Descy J-P, Gasol JM, Borges AV, Bouillon S, Darchambeau F (2014) Production of dissolved organic matter by phytoplankton and its uptake by heterotrophic prokaryotes in large tropical lakes. *Limnol Oceanogr* 59:1364–1375
- Morita RY (1982) Starvation-survival of heterotrophs in the marine environment. *Adv Microb Ecol* 6:171–198
- Pace ML, Cole JJ, Carpenter SR, Kitchell JF, Hodgson JR, van de Bogert C, Bade DL, Kritzberg ES, Bastviken D (2004) Whole-lake carbon-13 additions reveal terrestrial support of aquatic food webs. *Nature* 427:240–243
- Pace ML, Carpenter SR, Cole JJ, Coloso JJ, Kitchell JF, Hodgson JR, Middelburg JJ, Preston ND, Solomon CT, Weidel BC (2007) Does terrestrial organic carbon subsidize the planktonic food web in a clear-water lake? *Limnol Oceanogr* 52(5):2177–2189
- Raymond PA, Hartmann J, Lauerwald R, Sobek S, McDonald C, Hoover M, Butman D, Striegl RG, Mayorga E, Humborg C, Kortelainen P, Dürr H, Meybeck M, Ciais P, Guth P (2013) Global carbon dioxide emissions from inland waters. *Nature* 503:355–387
- Soetaert K, Hofmann AF, Middelburg JJ, Meysman FJR, Greenwood J (2007) The effect of biogeochemical processes on pH. *Mar Chem* 105:30–51
- Taipale SJ, Strandberg U, Peltomaa E, Galloway AWE, Ojala A, Brett MT (2013) Fatty acid composition as biomarkers of freshwater microalgae: analysis of 37 strains of microalgae in 22 genera and in seven classes. *Aquat Microb Ecol* 71:165–178
- Tranvik LJ, Downing JA, Cotner JB, Loiselle SA, Striegl RG, Ballatore TJ, Dillon P, Finlay K, Fortino K, Knoll LB, Kortelainen PL, Kutser T, Larsen S, Laurion I, Leech DM, Leigh McCallister SL, McKnight DM, Melack JM, Overholt E, Porter JA, Prairie Y, Renwick WH, Roland F, Sherman BS, Schindler DW, Sobek S, Tremblay A, Vanni MJ, Verschoor AM, von Wachenfeldt E, Weyhenmeyer GA (2009) Lakes and reservoirs as regulators of carbon cycling and climate. *Limnol Oceanogr* 65(6, part 2):2298–2314
- Van den Meersche K, Middelburg JJ, Soetaert K, van Rijswijk P, Boschker HTS, Heip CHR (2004) Carbon-nitrogen coupling and algal-bacterial interactions during an experimental bloom: Modeling a ^{13}C tracer experiment. *Limnol Oceanogr* 49(3):862–878
- van Gaever S, Moodley L, Pascotti F, Houtekamer M, Middelburg JJ, Danovaro R, Vanreusel A (2009) Trophic specialisation of metazoan meiofauna at the Håkon Mosby Mud Volcano: fatty acid biomarker isotope evidence. *Mar Biol* 156:1289–1296
- van Oevelen D, Moodley L, Soetaert K, Middelburg JJ (2006) The trophic significance of bacterial carbon in a marine intertidal sediment: results of an in situ stable isotope labeling study. *Limnol Oceanogr* 51(5):2349–2359
- Weyhenmeyer GA, Kosten S, Wallin MB, Tranvik LJ, Jeppesen E, Roland F (2015) Significant fraction of CO_2 emissions from boreal lakes derived from hydrologic inorganic carbon inputs. *Nat Geosci* 8:933–936
- White DC, David WM, Nickels JS, King JD, Bobbie RJ (1979) Determination of the sedimentary microbial biomass by extractable lipid phosphate. *Oecologia* 40:51–62
- White DC, Stair JO, Ringelberg DB (1996) Quantitative comparisons of in situ microbial biodiversity by signature biomarker analysis. *J Ind Microbiol* 17:185–196
- Wolf-Gladrow DA, Zeebe RE, Klaas C, Körtzinger A, Dickson AG (2007) Total alkalinity: the explicit conservative expression and its application to biogeochemical processes. *Mar Chem* 106:287–300

- Zeebe RE, Wolf-Gladrow DA (2001) In: Anonymous (ed) CO_2 in seawater: equilibrium, kinetics, isotopes. Elsevier
- Zelles L (1999) Fatty acid patterns of phospholipids and lipopolysaccharides in the characterisation of microbial communities in soil: a review. *Biol Fertil Soils* 29:111–129
- Zhang CL, Huang Z, Cantu J, Pancost RD, Brigmon RL, Lyons TW, Sassen R (2005) Lipid biomarkers and carbon isotope signatures of a microbial (*Beggiatoa*) mat associated with gas hydrates in the Gulf of Mexico. *Appl Environ Microbiol* 71(4):2106–2112